The Egyptian Journal of Radiology and Nuclear Medicine (2014) **45**, 1223–1231

Egyptian Society of Radiology and Nuclear Medicine

The Egyptian Journal of Radiology and Nuclear Medicine

www.elsevier.com/locate/ejrnm
www.sciencedirect.com

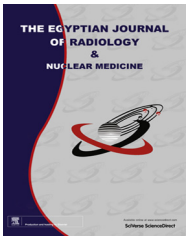

ORIGINAL ARTICLE

Diffusion tensor tractography as a supplementary tool to conventional MRI for evaluating patients with myelopathy

Amal Amin A. El Maati *, **Nivine Chalabi**

Department of Radiodiagnosis, Ain Shams University, Egypt

Received 12 July 2014; accepted 9 August 2014
Available online 2 September 2014

KEYWORDS

Cord myelopathy;
Spinal cord compression;
DTI;
ADC;
FA

Abstract *Purpose:* The aim of this study was to assess the clinical utility of DTI including apparent diffusion coefficient (ADC), fractional anisotropy (FA), in patients with symptoms of spinal cord myelopathy.

Patients and methods: Fifteen subjects with clinical symptoms of acute (n = 3) or slowly progressive (n = 12) spinal cord myelopathy and 11 healthy volunteers were prospectively selected. They all underwent magnetic resonance imaging of the spine at 3.0 T machine. In addition to conventional MRI, DTI was performed; maps of the apparent diffusion coefficient and of fractional anisotropy were reconstructed. Diffusion tensor tractography was used to visualize the morphological features of normal and impaired white matter at the level of the pathological lesions in the spinal cord. The patients were divided into two groups according to the signal intensity on T2WI (group A with no change in signal intensity and group B with high signal intensity).

Results: There were no statistically significant differences in the apparent diffusion coefficient and fractional anisotropy values between the different spinal cord segments of the normal subjects. All of the patients in group B had increased apparent diffusion coefficient values and decreased fractional anisotropy values at the lesion level compared to the normal controls. However, there were no statistically significant diffusion index differences between group A patients and the normal controls.

Conclusion: Diffusion tensor imaging is a reliable method for the evaluation of the diffusion properties of normal and compressed spinal cords. Furthermore, this technique can be used as an important supplementary tool to conventional MRI for the quantification of fiber damage in spinal cord compression, thus has the potential to be of great utility for treatment planning and follow up.

1. Introduction

Myelopathy describes any neurologic deficit related to the spinal cord. Myelopathy is usually due to compression of the

* Corresponding author.

Peer review under responsibility of Egyptian Society of Radiology and Nuclear Medicine.

http://dx.doi.org/10.1016/j.ejrnm.2014.08.004

spinal cord by osteophyte or extruded disk material in the cervical spine. Osteophytic spurring and disk herniation may also produce myelopathy localized to the thoracic spine, though less commonly. Other common sources of myelopathy are cord compression due to extradural mass caused by carcinoma metastatic to bone, and blunt or penetrating trauma. Many primary neoplastic, infectious, inflammatory, neurodegenerative, vascular, nutritional, and idiopathic disorders result in myelopathy (1). Clinically, the diagnosis of myelopathy depends on the neurologic localization of the finding to the spinal cord, rather than the brain or peripheral nervous system and then to a particular segment of the spinal cord. The antecedent clinical syndrome and other details of the patient's course are helpful, but imaging plays a crucial role. Clinical categories are based on the presence or absence of significant trauma or pain, and the mode of onset (slowly progressive or insidious onset versus stepwise progression versus sudden onset) (1).

Due to the high contrast obtained between different soft tissues, "conventional" (i.e. T1- and T2-weighted) magnetic resonance imaging (MRI) is the basic method for diagnosing spinal cord disorders. However, the signal of conventional MRI can be affected by many factors, including acquisition parameters (sequence type, TR, TE, flip angle, etc.), field strength, the water content of the spinal cord, and others. It can therefore neither directly depict the changes in the white matter fiber tracts nor assess the integrity of the spinal cord. Diffusion tensor imaging (DTI) is a noninvasive MRI technique that measures the random motion of water molecules and provides information about the cellular integrity and pathology of anisotropic tissues (2). Diffusion tensor imaging (DTI) can provide unique quantitative information on the microstructural features of white matter in the central nervous system (CNS) (2). Diffusion properties can be evaluated using quantitative indices such as the apparent diffusion coefficient (ADC) and the fractional anisotropy (FA). Furthermore, diffusion tensor tractography (DTT), another application of DTI, can be used to visualize the fiber tract pathways in vivo and can provide more direct information about the integrity of the tract (3). Although DTI has been successfully applied in brain research for decades (4), several main difficulties have hindered its extended utilization in spinal cord imaging, i.e. the small size of the spinal cord, movement artifacts (usually caused by cerebral spinal fluid pulsation, respiration and heart beat), regional magnetic heterogeneity, and a relatively long examination time (5–7). Several imaging techniques have been developed to solve these problems, e.g. multi-shot echo-planar imaging (MS-EPI), line scan imaging, parallel imaging, and the reversed gradient method (8–11). However, each of these techniques has its own inevitable drawbacks that can severely degrade the quality of DTI results. The single shot spin-echo echo-planar imaging (SS-SE-EPI) technique, the most popular diffusion imaging technique used in brain research, has several advantages including insensitivity to subject motion, fast acquisition time, and relatively high image quality (12–16). In this study, we chose SS-SE-EPI to evaluate the reliability of DTI in displaying and quantifying the fiber tract of the spinal cord. Several previous studies on 1.5T imaging have demonstrated that SS-SE-EPI DTI of the spinal cord is feasible (12–14,16). Quality improvements in spinal DTI might be further achieved with the use of a stronger magnetic field such as 3.0 T, which can dramatically improve the MRI signal, contrast and spatial resolution. However, DTI at higher field strength is more sensitive to susceptibility-induced image distortion and signal loss.

The aim of this study was to determine the suitability of spinal DTI for evaluating the degree of damage to the fiber tract in patients with cord myelopathy.

2. Patients and methods

This study included a total of 15 patients (eight men and seven women; mean age, 53.9 years) with clinical symptoms of spinal cord compression, who had been referred to the Misr Radiology center between March 2013 and April 2014, and underwent a combined multimodel imaging protocol comprising conventional MR imaging and DTI where maps of the apparent diffusion coefficient and of fractional anisotropy were reconstructed. Inclusion criteria matched clinical symptoms of acute or slowly progressive spinal cord compressions (focal sensory-motor deficit). Exclusion criteria were previous spine surgery, spine radiation therapy, and contraindication to MR imaging. Written informed consents were obtained from all patients before the study. As a control group, we enrolled 11 fully informed healthy volunteers (eight men and three women; mean age, 36.7 years) without neurologic disease.

3. MR imaging Technique

3.1. Image acquisition

The MRI data were obtained using a 3.0 T full-body system (Siemens Skyra) with a maximum gradient strength of 80 mT m^{-1} and a slew rate of 200 $Tm^{-1} s^{-1}$. The synergy cervical-thoracic-lumbar coil was equipped to receive the MR signal.

For all of the subjects, the MRI examination began with a sagittal T2-weighted fast spin-echo (FSE) sequence (FOV, 15.0 × 11.9 cm; image matrix, 128 × 82; section thickness, 2 mm; TR/TE, 2176/100 ms; echo train length, 15), a sagittal T1-weighted FSE sequence (FOV, 15.0 × 11.9 cm; image matrix, 232 × 146; section thickness, 2 mm; TR/TE, 430/6.9; echo train length, 4), and an axial T2-weighted FSE sequence (FOV, 15.0 × 15.0 cm; image matrix, 208 × 164; section thickness, 3 mm; TR/TE, 2493/120; echo train length, 29). Next, a sagittal spin-echo single-shot echoplanar (SE-SS-EPI) DTI that covered the lesions was acquired. The diffusion gradients were added in six non-collinear directions with a *b*-factor of 700 s/mm^2. The remaining imaging parameters were as follows: TR/TE, 5000/64 ms; FOV, 17.0 × 13.6 cm; image matrix, 96 × 61; 2-mm thickness and 0-mm gap. The voxel size was 1.56 × 1.94 × 2.00 mm. An enhanced T1WI sequence was obtained on the sagittal, axial and coronal planes after administering Gd-DTPA at a dose of 0.1 mmol/kg of Gadolinium that was injected automatically at a rate of 2 ml/s.

3.2. Image analysis

The ROIs were manually defined and measured on the FA maps with a rectangular area of approximately 16 mm^2. In the healthy volunteers, the ADC and FA values were measured at the disc levels (C2–C6 and T6–T11). Special attention was

paid to avoiding CSF partial-volume effects surrounding the cord, magnetic susceptibility effects, and motion artifacts in the ROIs. In the SCC subjects, ROIs with sizes nearly identical to those of the volunteers were placed at the compression sites. Two radiologists, both experienced in DTI analysis, independently drew the ROIs, and the mean values were used for further analysis.

3.3. Statistical analysis

The patients were divided into two groups based on the T2WI signal changes: group A were the patients without hyperintensity on T2WI and group B were the patients with hyperintensity on T2WI. We first investigated the FA and ADC differences among different spinal segments using a one-way analysis of variance (ANOVA). A post hoc analysis (the least-squares difference, LSD) was used to test for pairwise differences between segments when the ANOVA revealed significant differences. Furthermore, the diffusion indices (the FA and ADC values) were compared among the control, group A and group B using the methods described above. All of the statistical analyses were performed using SPSS 13.0 for Windows (SPSS Inc., Chicago, IL, USA). $P < 0.05$ was considered to be statistically significant.

4. Results

The FA and ADC values were successfully measured in healthy subjects and patients. In the healthy volunteers, the mean ADC and FA values for the cervical cord were $0.45 \pm 0.05 \times 10^{-3}$ mm^2/s and 0.75 ± 0.06, respectively. The mean ADC and FA values for the lower thoracic cord were $0.45 \pm 0.05 \times 10^{-3}$ mm^2/s and 0.74 ± 0.03, respectively. There were no statistically significant differences between the different cervical values ($P = 0.357$ for ADC and 0.464 for FA) and the lower thoracic spinal cord values ($P = 0.816$ for ADC and 0.711 for FA) (Table 1). Furthermore, there were also no significant differences between the cervical and lower thoracic cord values ($P = 0.745$ for ADC and 0.196 for FA).

There were no statistically significant differences in the spinal cord ADC or FA values between the control and group A patients ($P = 0.688$ for ADC; and $P = 0.242$ for FA). The ADC of group B was significantly higher than the controls ($P < 0.05$), and the FA was significantly lower (P, 0.05). There were also statistically significant ADC and FA differences between the A and B groups (both $P < 0.05$).

The ADC and FA means for the tumor subjects in group B were $0.730 \pm 0.217 \times 10^{-3}$ mm^2/s and 0.436 ± 0.247, respectively, which were not significantly different from those of the non-tumor subjects ($0.693 \pm 0.106 \times 10^{-3}$ mm^2/s and $0.434 + 0.136$, respectively) ($P = 0.539$). The ADC and FA means for the tumor subjects in group B were $0.472 \pm 0.107 \times 10^{3}$ mm^2/s and 0.704 ± 0.142, respectively, which were not significantly different from those of the non-tumor subjects ($0.463 \pm 0.062 \times 10^{-3}$ mm^2/s and $0.773 + 0.063$, respectively) ($P = 0.818$). However, there were statistically significant differences in the ADC or FA values between the group A and group B whatever the tumor or non-tumor subjects ($P < 0.05$). Eight patients had histologically proven spinal tumors: one pilocytic astrocytoma where the lesion is splaying apart the projectional fibers of the cord and with no pronounced infiltration or destruction in keeping with a low grade neoplastic lesion (Fig. 1), two intermediate grade astrocytomas with variable degrees of infiltration and fiber disruption clearly visible on tractograms (Fig. 2), three ependymomas with MR tractography show focal partial infiltration of the cord fibers specially at the solid enhancing part of the lesion (Fig. 3), two metastatic tumors with displacement of the fibres visible on the tractogram. Non-tumoral cases included two cases of degenerative arthritis with disk herniation, one spondylodiscitis with epidural abscess, two cases of multiple sclerosis and two cases of Devic's disease (neuromyelitis optica). It is noted that the lesions are not causing any infiltration or invasion of cord fibers in the tractogram (Fig. 4). Detailed results of the patients' data with estimates of ADC and FA on compression level are reported in Table 2.

Table 1 Comparison of FA and ADC values according to the level on healthy volunteers.

	Average	SD	*P* value
FA			
Cervical	0.75	0.06	0.464
Dorsal	0.74	0.03	0.711
ADC			
Cervical	0.45	0.05	0.357
Dorsal	0.45	0.05	0.816

5. Discussion

Unlike in DT imaging of the brain, single-shot echo planar DT imaging cannot be easily performed in the spinal cord (11). Diffusion tensor imaging of the spinal cord is limited by bony structures surrounding the spinal cord and the low signal-to-noise ratio. These difficulties were overcome by the advent of 3-T technologies and the development of new DT imaging protocols (11). Diffusion tensor imaging and DT imaging tractography have been used successfully in the spinal cord for assessing the disease burden in patients with MS (17), intramedullary tumors (14,18,19), and Wallerian degeneration associated with traumatic spinal cord injury and pontine infarction (20,21), as well as to assess recovery in patients with chronic spinal cord injury (22) and to evaluate motor functional outcome in patients with acute transverse myelitis (23). Intramedullary spinal cord tumors are rare lesions and account for 2–4% of all CNS tumors (24) representing approximately 20% of spine tumors in adults and up to 35% of spine tumors in children (25,26). By far, the most frequent intramedullary tumors in adults are ependymomas, which account for 60% of all intramedullary tumors, followed by astrocytomas, other gliomas, hemangioblastomas, and metastases, which are less frequent (25,27–31).

In this study, we chose single-shot spin-echo echo-planar imaging (SS-SE-EPI), the most popular diffusion imaging technique used in brain research, and evaluated the reliability of SS-SE-EPI DTI in displaying and quantifying the fiber tract of the spinal cord. The SS-SE-EPI sequence can be used to obtain DTI images with minimal influence from motion-induced artifacts such as respiratory, cardiac, and CSF pulsation (32–36). In accordance with several DTI and DTT in normal subjects previous studies on 1.5 T imaging, our findings on

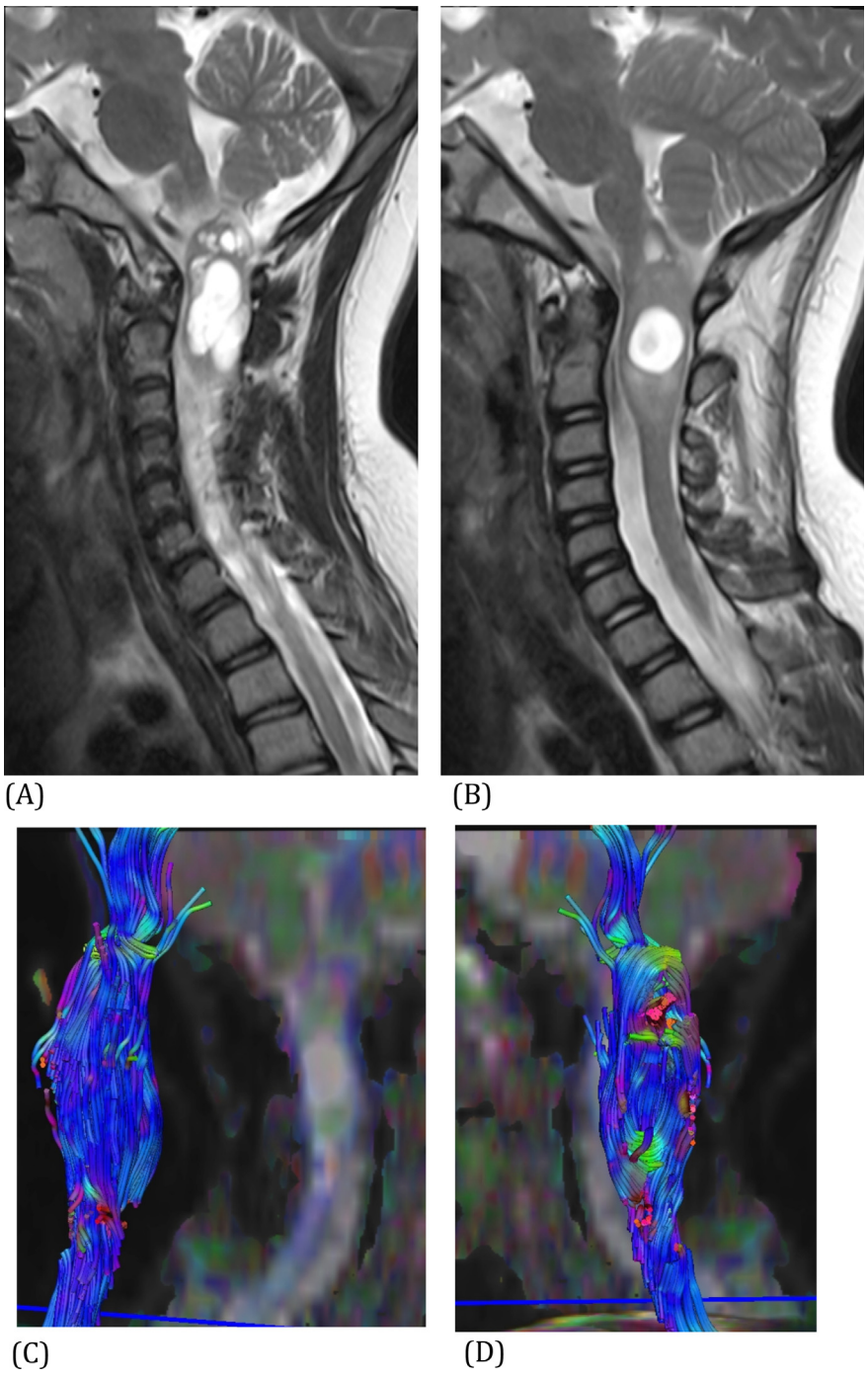

Fig. 1 Pilocytic astrocytoma in an 18 year old male patient with slowly progressive symptoms of spinal cord compression. (A) Sagittal T2 WI shows a moderate sized intramedullary space-occupying lesion within the upper most part of the cervical cord spanning the C1–C2 levels. This lesion has a mostly cystic septated well-defined component causing expansion of the cervical cord at that region. (B) Sagittal post contrast T1 WI shows an associated small solid intensely enhancing component along the superior left aspect of this cystic lesion. (C and D) MR tractography of the cord particularly emphasizing that such lesion is splaying apart the projectional fibers of the cord. The overall pattern as such confirms that this is a low-grade neoplastic lesion with no infiltration of destruction.

normal controls demonstrated that SS-SE-EPI DTI of the spinal cord can reliably visualize and quantify the diffusion properties of both the cervical and thoracic regions of the spinal cord.

The signal contribution by the 3.0 T MRI scanner used in this study allowed the imaging of much thinner sections (2 mm) than those reported in previous studies (4–5 mm) (5). As a result, partial-volume effects were dramatically decreased. Furthermore, we identified no serious artifacts (distorted or missing signal, etc.) that might have been caused by the high field strength used. Finally, rather than a b value of 1000 s/mm^2, which is widely used for brain DTI, we selected a b value of 700 s/mm^2 to increase the SNR of the diffusion images (8,9,36).

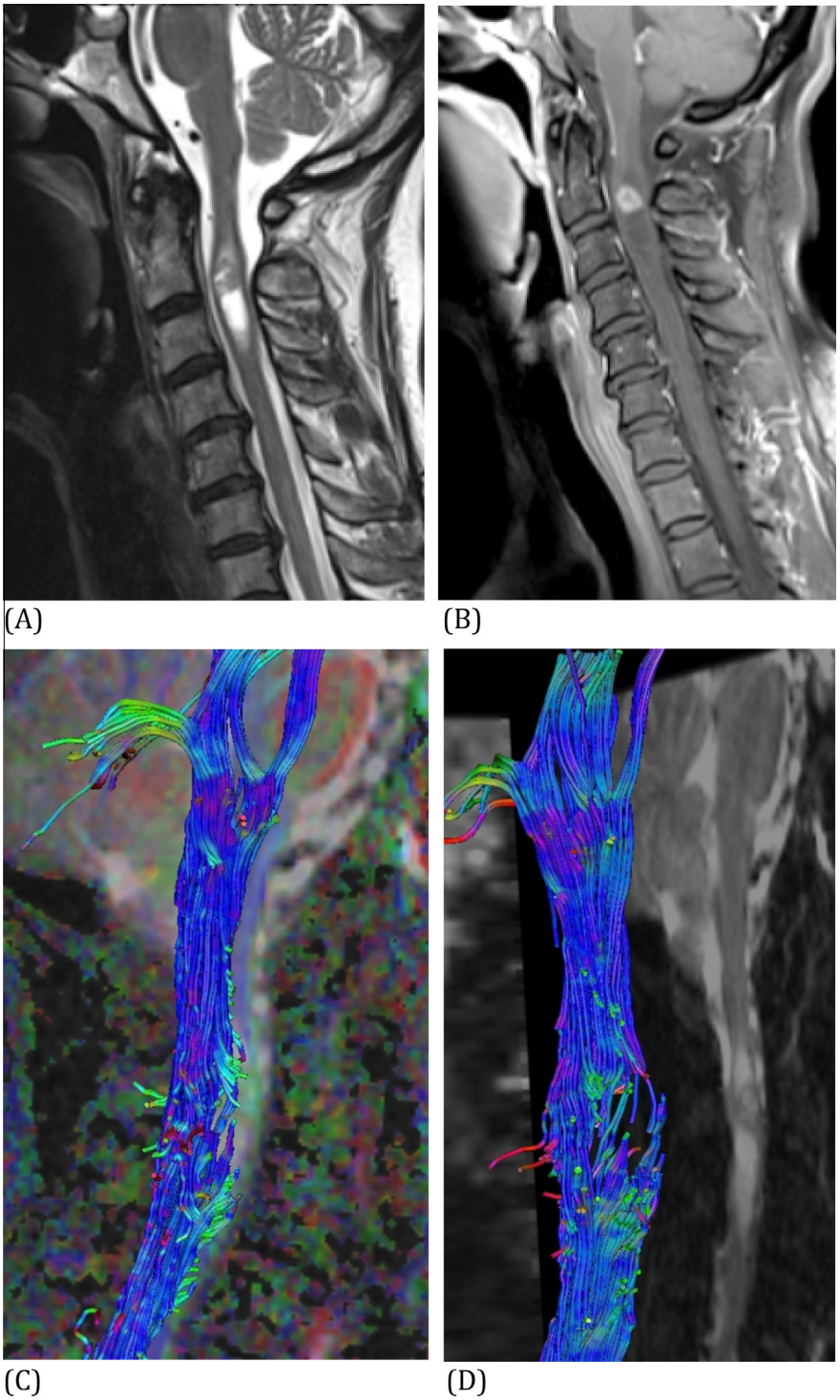

Fig. 2 Intermediate grade astrocytoma in a 50-year old female patient. (A and B) Sagittal T2WI and post contrast T1WI showed an intramedullary cervical cord space occupying lesion that causes focal cord expansion at its location opposite C2 and C3 levels. The lesion has predominantly cystic component which is non-enhancing and a small solid intensely heterogeneously enhancing component of about 1 cm opposite the C2–C3 disc which shows small area of breaking down at the center. (C and D) the fiber tracking of the projectional fibers of the brain stem and cord shows the implication of the tumorous lesion of the fibers at the C2 and C3 level is seen to cause variable degrees of infiltration and fiber disruption.

Concerning the DTI and DTT in normal subjects we observed no differences in the diffusion values between each imaging pair in the cervical and lower thoracic levels. Although several earlier studies demonstrated varying diffusion characteristics along the spinal cord (9,32), our findings are consistent with those of other research groups (14,37,38).

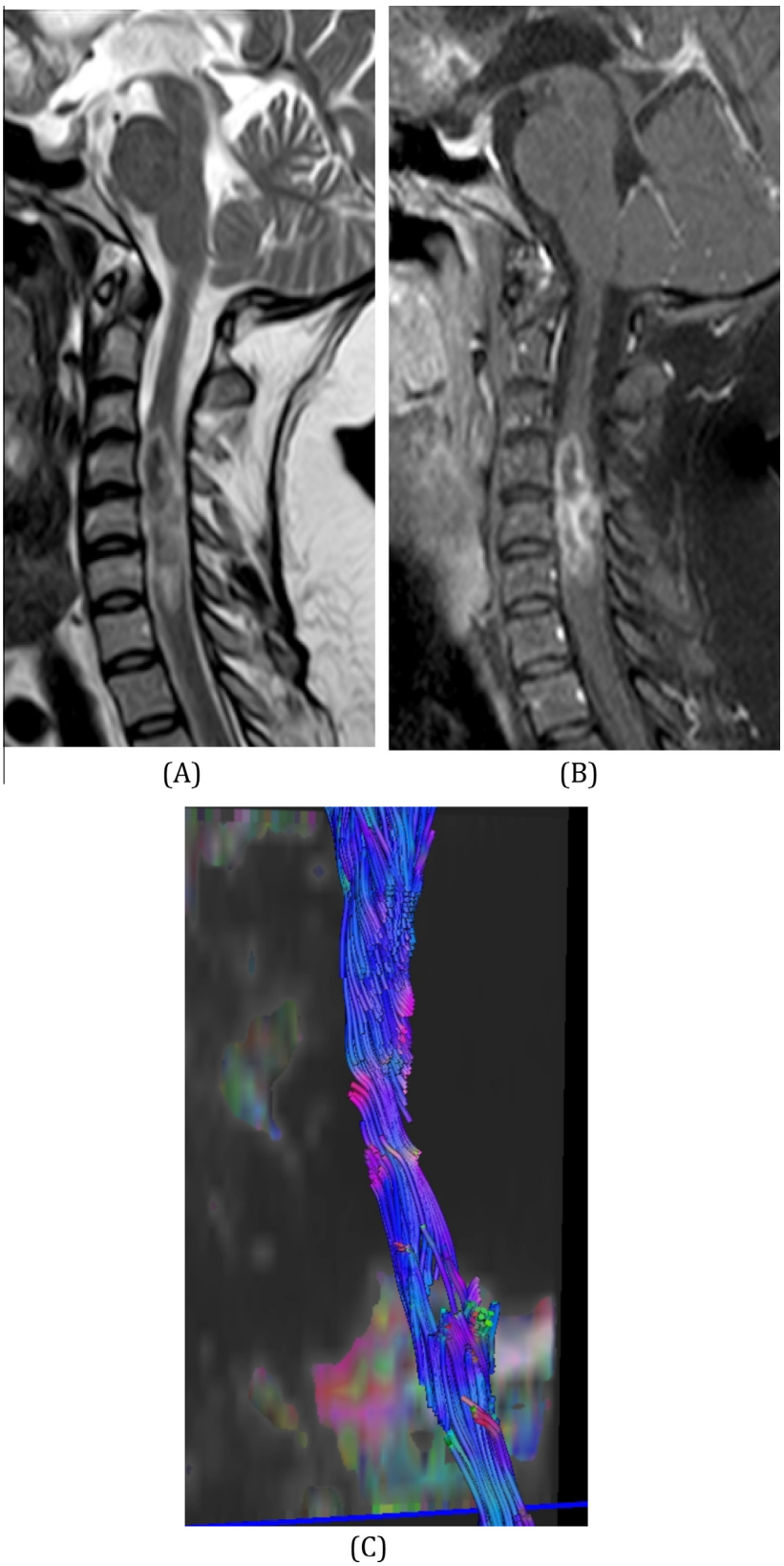

Fig. 3 Ependymoma in a 54 year old female patient. (A and B) Sagittal T2WI and post contrast T1WI revealed intra medullary lesion which is opposite C4, C5 and C6 levels and shows heterogenous hyperintense signal on T2WIs with hemorrhagic and necrotic components as well as solid enhancing components mostly marginal enhancement but also nodular enhancement at the lower aspect of the lesion. As regards the MR tractography (C) the lesion is seen to cause focal partial infiltration of such cord fibers particularly opposite which is pattern of malignant neoplasm.

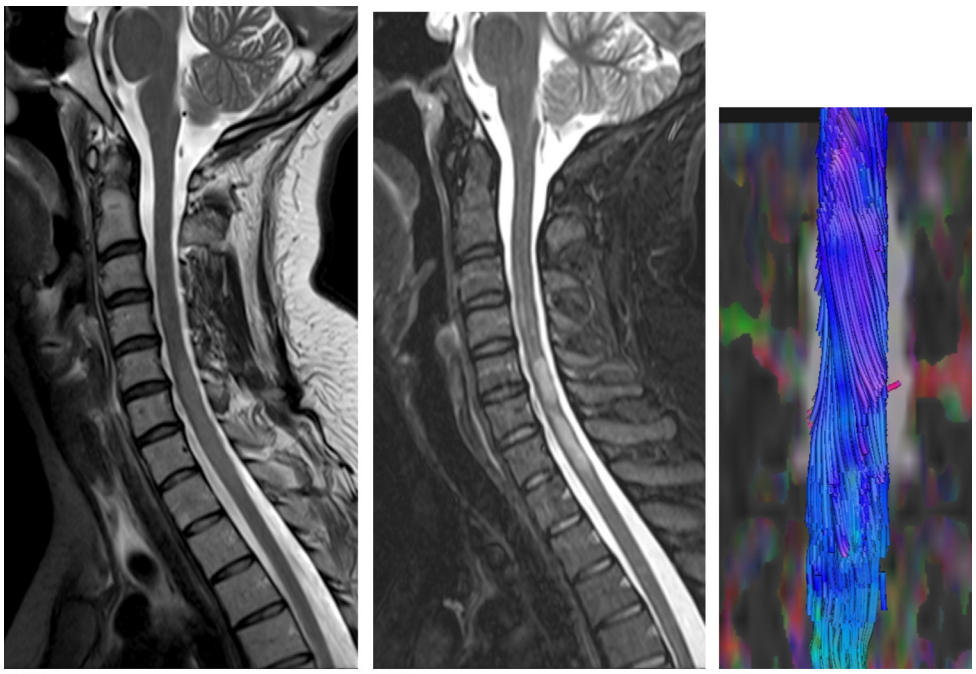

Fig. 4 Neuromyelitis optica in a 23 year-old female patient who presented with quadriparesis, more left than right. (A and B) sagittal T2WI and post contrast T1WI revealed intramedullary lesions, which spans C3 through D1 levels. They demonstrated hyperintense signal on T2 WI with homogenous post contrast enhancement. (C) Color coded projectional fibers for the cord showed that the lesions are not causing any infiltration or invasion of cord fibers, and this would be in keeping with demyelinating process rather than malignant neoplastic process.

This finding facilitates group comparisons in diffusion quantifications between damaged and normal sections of the spinal cord.

DTT of the neural fibers in the cervical spine has previously been investigated using a 3 T clinical magnetic resonance scanner (39). Consistent with previous reports, the tractograms of the complete cervical cord were well visualized in this study likely owing to the higher spatial resolution afforded by 3.0 T MRI.

In cervical spondylotic myelopathy group, which is the most common cause of spinal cord compression and results in cord demyelination, necrosis, and cavitation, our results confirmed increased ADC values and decreased FA values within the spinal cords of spinal cord compression patients presenting abnormally high signal intensities on T2WI. The changes in the diffusion indices of the lesions may reflect microstructural changes. An experimental study in rats found that decreased FA may be caused by mechanical disruption, fiber tearing and myelin sheaths, extracellular edema, Wallerian degeneration, demyelination, loss of spatial organization, liquefaction, and cystic degeneration (40). Demir et al. reported that DWI increased the sensitivity of MRI in depicting spinal cord changes in patients with clinical cervical spondylotic myelopathy symptoms (13). However, no marked anisotropy differences in the spinal cord were identified in the patients with light spinal cord compression (without a T2 high signal), which suggests that the microstructure of the spinal cord was not damaged in these patients.

Extramedullary intradural tumors can cause metastatic epidural spinal cord compression, which is defined radiographically as an epidural metastatic lesion causing true displacement of the spinal cord from its normal position in the spinal canal (41), and benign tumor SCC such as Schwannomas and meningiomas. Both damage the cord by direct compression, which causes demyelination and axonal damage, and by secondary vascular compromise. The early injury mechanism is vasogenic edema of the white matter (42). In this study, the patients in group B with spinal extramedullary intradural tumors had decreased FA values and increased ADC values at the affected spinal segments, which suggested fiber damage with or without local extracellular edema (43). This finding was coincident with a high T2WI signal intensity. However, the FA and ADC values in group A patients were within the normal range. The reason for this discrepancy may have been the adaptability of the spinal cord after chronic spinal cord compression.

The DTT technique facilitates the diagnosis of spinal cord abnormalities by allowing the clinician to locate the specific compression site. The DTT maps of the spinal cord compression patients in our study showed distortion and compression to different degrees but did not show obvious damage in the affected area of the spinal cord.

Regarding intramedullary lesions edema and fiber damage resulting in high-signal T2WI can be discriminated based on their diffusion properties (with edema, ADC increases dramatically, whereas FA decreases slightly; with fiber damage, FA decreases dramatically and ADC also increases significantly) (13,40). Our findings indicate that DTI not only can be used to quantify the diffusion properties of normal and compressed spinal cord but can also be used to visualize the fiber tract of the spinal cord in both normal and spinal cord compression subjects. DTT maps in the tumor group clearly indicated the

Table 2 Patients' data with results of the ADC and FA values on compression level.

	Age/sex	Pathology	Location	T2 SI	DTI findings	FA	ADC $\times 10^{-3}$ mm^2/s
1	33 F	Ependymoma	Cervical		Focal partial infiltration	308.2	2.497
2	33 F	Ependymoma	Cervical		Focal partial infiltration	344	2.355
3	60 M	Ependymoma	Cervical		Focal partial infiltration	247.7	1.216
4	16 M	Pilocytic astrocytoma	Upper Cervical		Splaying of fibers	194.5	1.628
5	63 M	Metastases	Dorsal		Displacement of fibers	345	1.107
6	50 F	Astrocytoma	Cervical		Infiltration and fiber disruption	161.3	1.082
7	54 M	Astrocytoma	Cervicodorsal		Infiltration and fiber disruption	625	1.102
8	56 M	Metastases	Dorsal		Displacement of fibers	161.3	1.082
9	45 M	Herniated disc	Cervical		Slight compression	625	1.102
10	56 M	Herniated disc	Dorsal		Slight compression	161.3	1.082
11	23 F	Neuromyelitis optica	Cervicodorsal		Change in color brightness	161.3	1.082
12	32 F	Neuromyelitis optica	Cervicodorsal		No infiltration	481	1.374
13	39 F	Multiple sclerosis	Cervical		No infiltration	673	1.506
14	36 F	Multiple sclerosis	Cervical		No infiltration	208.7	1.567
15	42 M	Spondylodiscitis with epidural abscess	Dorsal		Slight compression	600	0.851

relationship of the tumors, the degree of compression and the damage to the spinal cord which provides valuable information for surgical treatment.

Regarding patients with myelitis namely MS and neuromyelitis optica hyperintensities of the spinal cord represent a broad spectrum of lesions, from reversible to more severe lesions (44). DTI parameters are more sensitive than T2 signal analysis in assessing patients with myelitis (45). We observed lower FA and higher ADC values in patients with myelitis, as previously reported (36). Decrease in the FA values may reflect the degree of microstructural disorganization of the spinal cord, suggesting either local extracellular edema or a smaller number of fibers matching a larger extracellular space or both (45). In addition, radial diffusivity may serve as a marker of overall tissue integrity within chronic MS lesions (46). However, our results disagreed with a recent study done by Hodel et al. using a 3 T scanner for the assessment of the cervical spinal cord in patients with myelitis (44). They observed an increase in FA associated with a marked decrease in diffusivity values in patients with active lesions. Increased FA within gadolinium-enhancing lesions may be related to the resolution of edema and the inflammatory infiltrates.

In this study, we divided the patients into a normal signal group (group A) and a high-signal group (group B) based on the T2 signal. Significant differences in the diffusion indices (FA/ADC) were identified between group B and normal subjects, although there were no significant differences between group A and normal subjects. These findings suggested that the spinal fiber tract was severely damaged in group B but remained intact in group A, which, at a minimum, provided comparable evidence regarding the degree of damage to the spinal cord, as demonstrated by T2WI.

In conclusion, diffusion tensor imaging using the SS-SE-EPI technique at 3.0 T is a reliable method for the evaluation of the diffusion properties of normal and compressed spinal cords. Furthermore, this technique can be used as an important supplementary tool to conventional MRI for the quantification of fiber damage in patients with myelopathy.

Conflict of interest

None declared.

References

(1) Seidenwurm DJ. Myelopathy. Am J Neuroradiol 2008;29:1032–4.
(2) Clark CA, Werring DJ. Diffusion tensor imaging in spinal cord: methods and applications – a review. NMR Biomed 2002;15:578–86.
(3) Le Bihan D, Mangin JF, Poupon C, et al. Diffusion tensor imaging: concepts and applications. J Magn Reson Imaging 2001;13:534–46.
(4) Stieltjes B, Kaufmann WE, van Zijl PC, et al. Diffusion tensor imaging and axonal tracking in the human brainstem. Neuroimage 2001;14:723–35.
(5) Clark CA, Barker GJ, Tofts PS. Magnetic resonance diffusion imaging of the human cervical spinal cord in vivo. Magn Reson Med 1999;41:1269–73.
(6) Clark CA, Werring DJ, Miller DH. Diffusion imaging of the spinal cord in vivo: estimation of the principal diffusivities and application to multiple sclerosis. Magn Reson Med 2000;43:133–8.
(7) Cercignani M, Horsfield MA, Agosta F, et al. Sensitivity-encoded diffusion tensor MR imaging of the cervical cord. Am J Neuroradiol 2003;24:1254–6.
(8) Voss HU, Watts R, Ulug AM, et al. Fiber tracking in the cervical spine and inferior brain regions with reversed gradient diffusion tensor imaging. Magn Reson Imaging 2006;24:231–9.
(9) Wheeler-Kingshott CA, Hickman SJ, Parker GJ, et al. Investigating cervical spinal cord structure using axial diffusion tensor imaging. Neuroimage 2002;16:93–102.
(10) Robertson RL, Maier SE, Mulkern RV, et al. MR line-scan diffusion imaging of the spinal cord in children. Am J Neuroradiol 2000;21:1344–8.
(11) Tsuchiya K, Fujikawa A, Honya K, Nitatori T, Suzuki Y. Diffusion tensor tractography of the lower spinal cord. Neuroradiology 2008;50:221–5.
(12) Shanmuganathan K, Gullapalli RP, Zhuo J, et al. Diffusion tensor MR imaging in cervical spine trauma. Am J Neuroradiol 2008;29:655–9.
(13) Demir A, Ries M, Moonen CT, et al. Diffusion-weighted MR imaging with apparent diffusion coefficient and apparent diffusion tensor maps in cervical spondylotic myelopathy. Radiology 2003;229:37–43.
(14) Ducreux D, Lepeintre JF, Fillard P, Loureiro C, Tadié M, Lasjaunias P. MR diffusion tensor imaging and fiber tracking in 5 spinal cord astrocytomas. AJNR Am J Neuroradiol 2006;27:214–6.
(15) Nair G, Carew JD, Usher S, et al. Diffusion tensor imaging reveals regional differences in the cervical spinal cord in amyotrophic lateral sclerosis. Neuroimage 2010;53:576–83.

(16) Agosta F, Absinta M, Sormani MP, et al. In vivo assessment of cervical cord damage in MS patients: a longitudinal diffusion tensor MRI study. Brain 2007;130:2211–9.
(17) Ohgiya Y, Oka M, Hiwatashi A, Liu X, Kakimoto N, Westesson PL, et al. Diffusion tensor MR imaging of the cervical spinal cord in patients with multiple sclerosis. Eur Radiol 2007;17:2499–504.
(18) Ducreux D, Fillard P, Facon D, Ozanne A, Lepeintre JF, Renoux J, et al. Diffusion tensor magnetic resonance imaging and fiber tracking in spinal cord lesions: current and future indications. Neuroimaging Clin N Am 2007;17:137–47.
(19) Vargas MI, Delavelle J, Jlassi H, Rilliet B, Viallon M, Becker CD, et al. Clinical applications of diffusion tensor tractography of the spinal cord. Neuroradiology 2008;50:25–9.
(20) Guleria S, Gupta RK, Saksena S, Chandra A, Srivastava RN, Husain M, et al. Retrograde Wallerian degeneration of cranial corticospinal tracts in cervical spinal cord injury patients using diffusion tensor imaging. J Neurosci Res 2008;86:2271–80.
(21) Liang Z, Zeng J, Zhang C, Liu S, Ling X, Xu A, et al. Longitudinal investigations on the anterograde and retrograde degeneration in the pyramidal tract following pontine infarction with diffusion tensor imaging. Cerebrovasc Dis 2008;25:209–16.
(22) Ellingson BM, Ulmer JL, Kurpad SN, Schmit BD. Diffusion tensor MR imaging in chronic spinal cord injury. AJNR Am J Neuroradiol 2008;29:1976–82.
(23) Lee JW, Park KS, Kim JH, Choi JY, Hong SH, Park SH, et al. Diffusion tensor imaging in idiopathic acute transverse myelitis. AJR Am J Roentgenol 2008;191:W52–7.
(24) Stein BM, McCormick PC. Intramedullary neoplasms and vascular malformations. Clin Neurosurg 1992;39:361–87.
(25) Chang UK, Choe WJ, Chung SK, Chung CK, Kim HJ. Surgical outcome and prognostic factors of spinal intramedullary ependymomas in adults. J Neurooncol 2002;57:133–9.
(26) Raco A, Esposito V, Lenzi J, Piccirilli M, Delfini R, Cantore G. Long-term follow-up of intramedullary spinal cord tumors: a series of 202 cases. Neurosurgery 2005;56:972–81.
(27) Ferrante L, Mastronardi L, Celli P, Lunardi P, Acqui M, Fortuna A. Intramedullary spinal cord ependymomas—a study of 45 cases with long-term follow-up. Acta Neurochir (Wien) 1992;119:74–9.
(28) Lonser RR, Weil RJ, Wanebo JE, DeVroom HL, Oldfield EH. Surgical management of spinal cord hemangioblastomas in patients with von Hippel–Lindau disease. J Neurosurg 2003;98:106–16.
(29) Maira G, Amante P, Denaro L, Mangiola A, Colosimo C. Surgical treatment of cervical intramedullary spinal cord tumors. Neurol Res 2001;23:835–42.
(30) Miller DC. Surgical pathology of intramedullary spinal cord neoplasms. J Neurooncol 2000;47:189–94.
(31) Schick U, Marquardt G, Lorenz R. Intradural and extradural spinal metastases. Neurosurg Rev 2001;24:1–7.
(32) Ellingson BM, Ulmer JL, Kurpad SN, et al. Diffusion tensor MR imaging in chronic spinal cord injury. Am J Neuroradiol 2008;29:1976–82.
(33) Ellingson BM, Ulmer JL, Schmit BD. Morphology and morphometry of human chronic spinal cord injury using diffusion tensor imaging and fuzzy logic. Ann Biomed Eng 2008;36:224–36.
(34) Guleria S, Gupta RK, Saksena S, et al. Retrograde Wallerian degeneration of cranial corticospinal tracts in cervical spinal cord injury patients using diffusion tensor imaging. J Neurosci Res 2008;86:2271–80.
(35) Smith SA, Jones CK, Gifford A, et al. Reproducibility of tract-specific magnetization transfer and diffusion tensor imaging in the cervical spinal cord at 3 tesla. NMR Biomed 2010;23:207–17.
(36) van Hecke W, Nagels G, Emonds G, et al. A diffusion tensor imaging group study of the spinal cord in multiple sclerosis patients with and without T2 spinal cord lesions. J Magn Reson Imaging 2009;30:25–34.
(37) Facon D, Ozanne A, Fillard P, et al. MR diffusion tensor imaging and fiber tracking in spinal cord compression. Am J Neuroradiol 2005;26:1587–94.
(38) Ries M, Jones RA, Dousset V, et al. Diffusion tensor MRI of the spinal cord. Magn Reson Med 2000;44:884–92.
(39) Qin W, Yu CS, Zhang F, et al. Effects of echo time on diffusion quantification of brain white matter at 1.5 T and 3.0 T. Magn Reson Med 2009;61:755–60.
(40) Nevo U, Hauben E, Yoles E, et al. Diffusion anisotropy MRI for quantitative assessment of recovery in injured rat spinal cord. Magn Reson Med 2001;45:1–9.
(41) Gerszten PC, Welch WC. Current surgical management of metastatic spinal disease. Oncology (Williston Park) 2000;14:1013–24, discussion 1024, 1029–1030.
(42) Siegal T. Spinal cord compression: from laboratory to clinic. Eur J Cancer 1995;31:1748–53.
(43) Cole JS, Patchell RA. Metastatic epidural spinal cord compression. Lancet Neurol 2008;7:459–66.
(44) Hodel J, Besson P, Outteryck O, et al. Pulse-triggered DTI sequence with reduced FOV and coronal acquisition at 3 T for the assessment of the cervical spinal cord in patients with myelitis. AJNR 2013;34:676–82.
(45) Renoux J, Facon D, Fillard P, et al. MR diffusion tensor imaging and fiber tracking in inflammatory diseases of the spinal cord. AJNR Am J Neuroradiol 2006;27:1947–51.
(46) Klawiter EC, Schmidt RE, Trinkaus K, et al. Radial diffusivity predicts demyelination in ex vivo multiple sclerosis spinal cords. Neuroimage 2011;55:1454–60.